Costas Loop Lock Detection in the Advanced Receiver

A. Mileant
Telecommunications Systems Section

S. Hinedi
Communications Systems Research Section

The Advanced Receiver currently being developed uses a Costas digital loop to demodulate the subcarrier. Previous analyses of lock detector algorithms for Costas loops have ignored the effects of the inherent correlation between samples of the phase-error process. Accounting for this correlation is necessary to achieve the desired lock-detection probability for a given false-alarm rate. In this article, both analysis and simulations are used to quantify the effects of phase correlation on lock detection for the square-law and the absolute-value type detectors. Results are obtained which depict the lock-detection probability as a function of loop signal-to-noise ratio for a given false-alarm rate. The mathematical model and computer simulation show that the square-law detector experiences less degradation due to phase jitter than the absolute-value detector and that the degradation in detector signal-to-noise ratio is more pronounced for square-wave than for sine-wave signals.

I. Introduction

Costas loops are being used extensively in modern coherent communication systems to track both subcarriers and suppressed carriers. In many applications, residual carriers are being replaced by suppressed carriers as the latter dedicates the total transmitted power to both carrier tracking and symbol detection simultaneously. This has a clear advantage over residual carrier tracking, which requires a fraction of the total transmitted power delegated solely to that purpose, and hence, reduces the available power that can be used for symbol detection. The disadvantages of Costas loops are that they require symbol synchronization and suffer from an additional loss factor typically referred to as squaring loss, which is highly dependent on symbol energy-to-noise ratio. Squaring loss is the result of forming the product of the inphase and quadrature signals to wipe out the data modulation, in order to obtain a feedback error signal that is only a function of the instantaneous phase error [1]. Another disadvantage of suppressed carrier tracking is the issue of false lock, which occurs either as a result of accumulated delay [2] or during acquisition with frequency uncertainty greater than one-half the symbol rate [3, 4]. The latter can be detected through a false-lock indicator, as described in [3].

Lock detection is an important part of a tracking loop's operation and monitoring, as it provides an insight

into the tracking loop's behavior in real time. Lock detection basically serves as a binary indicator of whether the loop is tracking the received signal or not, and during loop start-up it also indicates whether or not the loop has acquired the phase of the signal. There are mainly two kinds of lock detectors for Costas loops, the $I^2 - Q^2$, or square-law detector, and the $| I | - | Q |$, or absolute-value detector [5]. Both have been analyzed in the past at high loop signal-to-noise ratio (SNR), which basically assumes zero phase-tracking error. At low loop SNR, the assumption of zero phase jitter becomes inadequate and results in system operating parameters that are different from their design counterparts. Thus, a new model is required which has to account for the phase jitter and the correlation between samples of the phase-error process. The latter is essential in an accurate performance prediction analysis, in order to operate the system at the desired lock-detection probability for a given false-alarm rate. The analysis of the detectors, including the phase correlation and assuming either a sinusoidal or a square wave signal, is presented in Section II. In the case of a square-wave, the analysis is general and includes any windowing operation as described in [6]. The discussion of the results and some simulated data are shown in Section III, followed by the conclusion in Section IV.

II. Lock-Detection Analysis

Suppressed carrier tracking for binary-phase shift keyed (BPSK) signals can be accomplished using a squaring loop or a Costas loop [7]. The squaring loop relies on wiping out the data by a squaring operation and tracking the resulting residual double-frequency component with a classical phase-locked loop. The squaring loop does not require symbol timing, but results in an additional noise term which becomes dominant at low SNR. On the other hand, the Costas loop implements a phase discriminator by forming the product of the inphase and quadrature signals. That too results in some degradation, commonly referred to as the squaring loss. Depending on the design, both loops can be implemented with identical performances for all practical purposes. The Costas loop has various derivatives, each approximating the maximum a posteriori (MAP) estimator at different SNRs [8]. For example, a hard-limiter can be included in the inphase arm to estimate the current symbol, and that results in less squaring loss at high SNRs.

This article is concerned with the lock detection for the all-digital IQ loop, which is also a derivative of the Costas loop with integrate-and-dump arm filters. All-digital refers to the fact that the input waveform to the loop is a sequence of samples and that the integrate-and-dump arm filters are digital accumulators. The IQ loop and square-law lock detector are depicted in Fig. 1 for the square-wave case, with the optional windowing operation on the quadrature channel. The analysis that follows will be applicable for both sinusoidal and square waves. The received waveform is digitized to produce the samples r_j, which are subsequently digitally mixed with the inphase and quadrature references. The outputs of the mixers, running at the sampling rate, are accumulated to detect the received symbols. It is assumed that there are L samples per symbol and that perfect symbol synchronization has been achieved. The accumulator outputs, now at the symbol rate, are multiplied together to wipe out the data and again accumulated to reduce the processing rate even further. The output, running at a new rate (referred to as the loop update rate), is the input to the digital loop filter which provides a frequency estimate to adjust the phase of the numerically controlled oscillator (NCO). The lock detector processes the arm accumulator outputs at the symbol rate, accumulates the result over M symbols, and provides a binary decision on the loop status.

In the I and Q branches of Fig. 1, the signals accumulated over L samples during the kth symbol interval are given by

$$x_{Ik} = d_k L\sqrt{P_D}\,\omega_k + n_{Ik} \qquad k = 1, \ldots, M$$

and (1)

$$x_{Qk} = d_k L\sqrt{P_D}\,v_k + n_{Qk} \qquad k = 1, \ldots, M$$

where

$$\omega_k = \left(1 - | u_k |\right), \quad u_k = \frac{2}{\pi}\phi_k, \quad | \phi_k | \leq \pi$$

$$v_k = \begin{cases} u_k & | \phi_k | \leq \pi W/2 \\ \mathrm{sgn}(\phi_k)W & \pi W/2 \leq | \phi_k | \leq \pi(1 - W/2) \\ 2\mathrm{sgn}(\phi_k) - u_k & \pi(1 - W/2) \leq | \phi_k | \leq \pi \end{cases} \tag{2}$$

for a square-wave subcarrier and

$$\omega_k = \cos\phi_k$$

$$v_k = \begin{cases} \sin\phi_k & | \phi_k | \leq \pi W/2 \\ \sin(\phi_k W) & \pi W/2 \leq | \phi_k | \leq \pi(1 - W/2) \\ \sin\phi_k & \pi(1 - W/2) \leq | \phi_k | \leq \pi \end{cases} \tag{3}$$

for a sine-wave subcarrier, where P_D is the average data power, d_k is the data value of the kth binary symbol (± 1 equally likely), ϕ_k is the subcarrier phase-estimation error (radians) at time k, W is the width of the window in the Q channel (i.e., the fraction of cycle of the reference signal which has nonzero value $W \leq 1$ [$W = 1$ means no window is used]), and n_{Ik}, n_{Qk} are zero-mean white Gaussian noise samples. From Eq. (1), the mean values and the variances of x_{Ik} and x_{Qk} conditioned on ϕ_k and d_k are given by

$$\mu_{Ik} = d_k L\sqrt{P_D}\,\omega_k \qquad \sigma_I^2 = L\sigma_n^2$$

and (4)

$$\mu_{Qk} = d_k L\sqrt{P_D}\,v_k \qquad \sigma_Q^2 = WL\sigma_n^2$$

where $\sigma_n^2 = N_0 B_n$ is the noise variance of a received sample, N_0 is the one-sided noise spectral density, and B_n is the Nyquist bandwidth. The equations that follow are applicable to both sine and square waves.

A. Square-Law Detector

The first algorithm considered detects the in-lock state by producing a signal that is proportional to the cosine of the phase error (in the case of a sinusoidal wave) and averaging it over several symbols before comparing it to a threshold τ. Referring to Fig. 1,

$$\sum_{k=1}^{M} y_k \gtrless \tau, \quad \text{where} \quad y_k \triangleq x_{Ik}^2 - x_{Qk}^2 \tag{5}$$

An estimation of the performance of this lock detector requires the first and second moments of x_{Ik}^2 and x_{Qk}^2 conditioned on ϕ_k, which are readily obtainable:

$$\overline{x_{Ik}^2} = \mu_{Ik}^2 + \sigma_I^2 \tag{6a}$$

$$\overline{x_{Qk}^2} = \mu_{Qk}^2 + \sigma_Q^2 \tag{6b}$$

$$\overline{x_{Ik}^4} = \mu_{Ik}^4 + 6\mu_{Ik}^2\sigma_I^2 + 3\sigma_I^4 \tag{7a}$$

$$\overline{x_{Qk}^4} = \mu_{Qk}^4 + 6\mu_{Qk}^2\sigma_Q^2 + 3\sigma_Q^4 \tag{7b}$$

where μ_{Ik}, μ_{Qk}, σ_I^2, and σ_Q^2 are given by Eq. (4). Using Eqs. (6) and (7), the variances of x_{Ik}^2 and x_{Qk}^2 become respectively

$$\text{var}(x_{Ik}^2) = 4\mu_{Ik}^2\sigma_I^2 + 2\sigma_I^4 \tag{8a}$$

and

$$\text{var}(x_{Qk}^2) = 4\mu_{Qk}^2\sigma_Q^2 + 2\sigma_Q^4 \tag{8b}$$

The mean value of y_k is obtained from Eqs. (4) and (6) in Eq. (5), namely

$$\mu_{y_k} = L^2 P_D(\omega_k^2 - v_k^2) + L\sigma_n^2(1 - W)$$

The variance of y_k, $\sigma_{y_k}^2$, will be the sum of variances of x_{Ik}^2 and x_{Qk}^2, and is obtained by using Eq. (4) in Eq. (8), i.e.,

$$\sigma_{y_k}^2 = 2L^2\sigma_n^4\left[\frac{2LP_D}{\sigma_n^2}(\omega_k^2 + Wv_k^2) + 1 + W^2\right]$$

The lock-detector signal z is the accumulation of My_k samples, which are highly correlated due to the phase-error samples. The mean value and variance of z, μ_z, and σ_z^2 are derived in the Appendix, where it is shown that

$$\mu_z = M\Big(L^2 P_D d + L\sigma_n^2(1 - W)\Big) \tag{9}$$

and

$$\sigma_z^2 = M^2L^4P_D^2(g - d^2) + 4ML^3P_D\sigma_n^2(f + hW)$$

$$+ 2ML^2\sigma_n^4(1 + W^2) \tag{10}$$

The parameters d, f, h, and g depend on the waveform type and are given by ($b \triangleq W\pi/2$)

$$d \simeq 1 - 2\left(\frac{2}{\pi}\right)^{1.5}\sigma_\phi$$

$$f = \left(1 - \frac{4}{\pi}\overline{|\phi|} + \frac{4}{\pi^2}\overline{\phi^2}\right)$$

$$h = \frac{4}{\pi^2}\overline{\phi^2}$$

$$g = 1 - \frac{8}{\pi}\overline{|\phi|} + \left(\frac{4}{\pi}\right)^2\frac{1}{M^2}\sum_{k=0}^{M-1} c(k)d(k)$$

where

$$\overline{|\phi|} \simeq \sqrt{\frac{2}{\pi}}\sigma_\phi$$

and

$$\overline{\phi^2} \simeq \sigma_\phi^2 \ \text{erf}\left(\frac{b}{\sqrt{2\sigma_\phi^2}}\right)$$

$$\sigma_\phi^2 = \left(\frac{\pi}{2}\right)^2 W\left(\frac{N_0 B_{sc}}{P_D}\right)\left(1 + \frac{1}{2E_s/N_0}\right) \qquad (11)$$

for a square-wave subcarrier, and

$$d = \exp(-2\sigma_\phi^2)$$

$$f = 0.5\left(1 + \exp(-2\sigma_\phi^2)\right)$$

$$h = 0.5\Big(1 - \exp(-2\sigma_\phi^2)\Big)$$

$$g = \frac{1}{M^2}\sum_{k=0}^{M-1} c(k)d(k)$$

$$\sigma_\phi^2 = \left(\frac{N_0 B_{sc}}{P_D}\right) W\left(1 + \frac{1}{2E_s/N_0}\right) \qquad (12)$$

for a sine-wave subcarrier. Note that Eqs. (11) and (12) specify the variance of the phase jitter, assuming the linear loop model. For example, at 15 dB of nominal loop SNR, the actual variance σ_ϕ^2 can be about 1 dB larger. Nominal loop SNR ρ is defined as $1/\sigma_\phi^2$, where σ_ϕ^2 is obtained from the linear model; B_{sc} is the one-sided noise bandwidth of the Costas loop, and E_s/N_0 is the symbol energy-to-noise ratio. The constants $c(k)$ and $d(k)$ are defined as follows:

$$c(k) = \begin{cases} M & \text{for } k = 0 \\ 2(M-k) & \text{for } k = 1, 2, \ldots, M-1 \end{cases}$$

for both waveforms, but

$$d(k) \triangleq \int_{-b}^{b}\int_{-b}^{b} \mid \phi_1 \mid\mid \phi_2 \mid p(\phi_1, \phi_2, \tau_k)d\phi_1 d\phi_2$$

for a square wave and

$$d(k) = \begin{cases} 0.5\Big(1 + \exp(-2\sigma_\phi^2)\Big) & \text{for } k = 0 \\ \exp(-4\sigma_\phi^2)\cosh\Big(2\sigma_\phi^2 C(\tau_k)\Big) & k = 1, 2, \ldots, M-1 \end{cases}$$

for a sine wave; $C(\tau_k)$ is the correlation function of the phase-error process in the tracking loop, which is assumed to be of the form given by Eq. (A-9) [9], and the second-order joint probability density function of the correlated phase process $p(\phi_1, \phi_2, \tau_k)$ is assumed as in Eq. (A-10). When the loop is in-lock and assuming high loop SNR, $\phi_k \to 0$ for all k. Hence $\omega_k^2 \to 1$ and $v_k^2 \to 0$, and the above mean value and variance of the detector's signal simplify to

$$\mu_z = M\Big(L^2 P_D + L\sigma_n^2(1 - W)\Big)$$

$$\sigma_z^2 = 4ML^2\sigma_n^4\left[\frac{LP_D}{\sigma_n^2} + \frac{1 + W^2}{2}\right]$$

which are true for both square-wave and sine-wave signals. Note that in the above equation the following relation holds:

$$\frac{LP_D}{\sigma_n^2} = \frac{2E_s}{N_0}$$

because $L = 2T_s B_n$ (Nyquist sampling), where T_s is the symbol time, $\sigma_n^2 = N_0 B_n$, and $T_s P_D = E_s$, the energy per symbol.

B. Absolute-Value Detector

For the absolute-value detector, the squaring operation in Fig. 1 is replaced by an absolute-value operation, and the algorithm defining the new lock detector becomes

$$\sum_{k=1}^{M} y_k \gtrless \tau, \quad \text{where} \quad y_k \triangleq \mid x_{Ik} \mid - \mid x_{Qk} \mid \qquad (13)$$

In order to estimate the performance of this lock detector, the first and second moments of $\mid x_{Ik} \mid$ and $\mid x_{Qk} \mid$ are needed, again assuming a white Gaussian noise process at

the phase-locked loop input. These moments, conditioned on ϕ_k, become

$$\begin{aligned}\overline{|\,x_{Ik}\,|} &\triangleq r_{Ik} \\ &= L\sqrt{P_D}\,\omega_k \operatorname{erf}\left(\sqrt{\frac{E_s}{N_0}\,\omega_k^2}\right) \\ &\quad + \sqrt{\frac{2L}{\pi}}\,\sigma_n \exp\left(-\frac{E_s}{N_0}\,\omega_k^2\right) \\ \overline{|\,x_{Qk}\,|} &\triangleq r_{Qk} \\ &= L\sqrt{P_D}\,v_k \operatorname{erf}\left(\sqrt{\frac{E_s v_k^2}{N_0 W}}\right) \\ &\quad + \sqrt{\frac{2LW}{\pi}}\,\sigma_n \exp\left(-\frac{E_s}{N_0}\,\frac{v_k^2}{W}\right)\end{aligned} \tag{14}$$

The second moments of $|\,x_{Ik}\,|$ and $|\,x_{Qk}\,|$ are identical to the second moments of x_{Ik} and x_{Qk}, and are given by Eq. (6). The mean value of y_k follows from Eqs. (13) and (14):

$$\begin{aligned}\mu_{yk} &\triangleq r_{Ik} - r_{Qk} \\ &= L\sqrt{P_D}\left(\omega_k \operatorname{erf}\left(\sqrt{\frac{E_s}{N_0}\,\omega_k^2}\right) - v_k \operatorname{erf}\left(\sqrt{\frac{E_s v_k^2}{N_0 W}}\right)\right) \\ &\quad + \sqrt{\frac{2L}{\pi}}\,\sigma_n\left(\exp\left(-\frac{E_s}{N_0}\,\omega_k^2\right) - \sqrt{W}\exp\left(-\frac{E_s}{N_0}\,\frac{v_k^2}{W}\right)\right)\end{aligned} \tag{15}$$

and the variance of y_k is

$$\sigma_{yk}^2 = L^2 P_D\left(\omega_k^2 + v_k^2\right) + L\sigma_n^2(1+W) - \left(\overline{r_{Ik}}^2 + \overline{r_{Qk}}^2\right)$$

The lock detector's signal z is again obtained by adding My_k samples. The mean and variance of z are found by averaging the first two moments of z over the correlated phase process in the tracking loop. This is carried out in the Appendix and gives

$$\begin{aligned}\mu_z &= M\mu_y \\ &= M\left[L\sqrt{P_D}\left(\overline{\omega \operatorname{erf}\left(\sqrt{\frac{E_s}{N_0}\,\omega^2}\right)} - \overline{v \operatorname{erf}\left(\sqrt{\frac{E_s v^2}{N_0 W}}\right)}\right)\right. \\ &\quad \left. + \sqrt{\frac{2L}{\pi}}\,\sigma_n\left(\overline{\exp\left(-\frac{E_s}{N_0}\,\omega^2\right)} - \sqrt{W}\,\overline{\exp\left(-\frac{E_s}{N_0}\,\frac{v^2}{W}\right)}\right)\right]\end{aligned} \tag{16}$$

$$\begin{aligned}\sigma_z^2 &= M\left(L^2 P_D\left(\overline{\omega^2} + \overline{v^2}\right) + L\sigma_n^2(1+W)\right) \\ &\quad + \sum_{\substack{\text{all } i,j \\ i \neq j}}\sum\left(\overline{r_{Ii}r_{Ij}} + \overline{r_{Qi}r_{Qj}}\right) - M^2\left(\overline{r_I}^2 + \overline{r_Q}^2\right)\end{aligned} \tag{17}$$

The bar over the product terms denotes expectation over the joint probability density function of ϕ_i, ϕ_j, assumed to be of the form given by Eq. (A-10), and r_{Ik}, r_{Qk} are defined by Eq. (14). Because no closed-form solutions for the above averaging operations are known, the averaging was done numerically. When the loop is in-lock and at high loop SNR, $\phi_k \to 0$ for all k. Hence, $\omega_k^2 \to 1$ and $v_k^2 \to 0$, and the above mean value and variance of the lock detector simplify to

$$\begin{aligned}\mu_z &= M\left[L\sqrt{P_D}\,\operatorname{erf}\left(\sqrt{\frac{E_s}{N_0}}\right)\right. \\ &\quad \left. + \sqrt{\frac{2L}{\pi}}\,\sigma_n\left(\exp\left(-\frac{E_s}{N_0}\right) - \sqrt{W}\right)\right]\end{aligned} \tag{18}$$

$$\begin{aligned}\sigma_z^2 &= M\left[L^2 P_D + L\sigma_n^2(1+W)\right. \\ &\quad - \left(L\sqrt{P_D}\,\operatorname{erf}\left(\sqrt{\frac{E_s}{N_0}}\right) + \sqrt{\frac{2L}{\pi}}\,\sigma_n \exp\left(-\frac{E_s}{N_0}\right)\right)^2 \\ &\quad \left. - \frac{2WL}{\pi}\,\sigma_n^2\right]\end{aligned} \tag{19}$$

C. Probability of Detection and of False Indication

During subcarrier detection, each z sample is compared with a predefined threshold τ, and the lock detector decides that the loop is in-lock when $z > \tau$. It is possible that even when no signal is present, z will occasionally be larger than τ. In this case, the lock detector will mistakenly declare an in-lock condition. The probability of false indication is

$$P_f = \frac{1}{\sqrt{2\pi\sigma_{z0}^2}} \int_{\tau}^{\infty} \exp\left(-\frac{(z-\mu_{z0})^2}{2\sigma_{z0}^2}\right) dz$$

$$= \frac{1}{2}\,\mathrm{erfc}\left(\frac{\tau-\mu_{z0}}{\sqrt{2\sigma_{z0}^2}}\right) \tag{20}$$

where μ_{z0} and σ_{z0}^2 are the mean and variance of the lock-detector signal in the out-of-lock state, and $\mathrm{erfc}(x)$ is the complementary error function ($\mathrm{erfc}(x) = 1 - \mathrm{erf}(x)$, where $\mathrm{erf}(x)$ is the error function defined in the Appendix). For the square-law detector, μ_{z0} and σ_{z0}^2 are obtained from Eqs. (9) and (10) by making $P_D = 0$ (or, equivalently, assuming that $\overline{\omega_k}$ and $\overline{v_k}$ in Eq. 4 are zero), namely

$$\mu_{z0} = ML\sigma_n^2(1-W)$$

$$\sigma_{z0}^2 = 2ML^2\sigma_n^4(1+W^2)$$

whereas for the absolute-value detector, Eqs. (18) and (19) result in

$$\mu_{z0} = M\sqrt{\frac{2L}{\pi}}\,\sigma_n\left(1-\sqrt{W}\right)$$

$$\sigma_{z0}^2 = ML\sigma_n^2\left(1-\frac{2}{\pi}\right)(1+W) \tag{21}$$

Given a desired probability of false indication P_f, the threshold τ is obtained by solving Eq. (20) and setting it equal to

$$\tau = \sqrt{2\sigma_{z0}^2}\;\mathrm{erfc}^{-1}\,(2P_f) + \mu_{z0} \tag{22}$$

where $\mathrm{erfc}^{-1}(\cdot)$ is the inverse complementary error function. When the loop is in-lock, it can be argued via the central limit theorem that the random variable z is approximately Gaussian, with mean and variance obtained earlier for either the square-law or the absolute-value detector. For either detector, the probability of detection is

$$P_d = \frac{1}{\sqrt{2\pi\sigma_z^2}} \int_{\tau}^{\infty} \exp\left(-\frac{(z-\mu_z)^2}{2\sigma_z^2}\right) dz$$

$$= \frac{1}{2}\,\mathrm{erfc}\left(\frac{\tau-\mu_z}{\sqrt{2\sigma_z^2}}\right)$$

where μ_z and σ_z^2 are given by Eqs. (9) and (10) or by Eqs. (16) and (17). Defining the detector's SNR as

$$\mathrm{SNR}_z \triangleq \frac{\mu_z^2}{\sigma_z^2} \tag{23}$$

then, for $\mu_{z0} = 0$ ($W = 1$), the probability of detection in terms of SNR_z can be expressed as

$$P_d = \frac{1}{2}\;\mathrm{erfc}\left(\frac{\sigma_{z0}}{\sigma_z}\;\mathrm{erfc}^{-1}\,(2P_f) - \sqrt{\frac{\mathrm{SNR}_z}{2}}\right)$$

The above equation shows the dependence of the probability of detection on the detector's SNR. Phase jitter in the tracking loop degrades the detector's SNR by a factor D:

$$D = \mathrm{SNR}_z/\mathrm{SNR}_{z\,(ideal)} \tag{24}$$

where $\mathrm{SNR}_{z\,(ideal)}$ is the detector SNR, assuming infinite loop SNR, i.e., no phase jitter. $\mathrm{SNR}_{z\,(ideal)}$ is computed from Eq. (23) using the high-SNR expressions in Eqs. (18) and (19) for μ_z and σ_z^2. For a given W, M, loop SNR ρ ($\rho = 1/\sigma_\phi^2$ where σ_ϕ^2 is given by Eq. 11 or 12 repectively), and P_f, the detector's SNR must be increased approximately by the factor $1/D$ in order to achieve a desired probability of detection.

III. Discussion and Numerical Results

Computer simulation was performed in order to check the predictions of the analysis. Figure 2 depicts the probability of lock detection versus symbol energy-to-noise ratio E_s/N_0 for both sine-wave and square-wave signals, assuming ideal conditions, i.e., no phase jitter in the tracking loop. The square-law detector performs slightly better than the absolute-value detector for a given symbol SNR.

The degradation in detection probability for a finite-loop SNR is shown in Figs. 3(a) and 3(b) for the square-law and absolute-value detectors, respectively. The threshold

τ was set to achieve probabilities of false detection P_f of 10^{-1} and 10^{-4}, and detector SNR was set to achieve nominal probabilities of detection $\overline{P_d}$ of 0.99 and 0.90. Nominal probability refers to the case of no phase jitter in the loop. It is clear that sine waves produce less degradation than square waves, and this is true for both detection schemes.

The performance of both detectors is compared in Fig. 4 for square-wave signals only, since the difference in performance is almost negligible for sine-wave signals. The performance with respect to detector SNR is shown in Fig. 5 for a 15-dB loop SNR. The improvement in detection probability due to windowing is clear for both detectors and can result in several decibels. Finally, Fig. 6 depicts both theoretical and simulation points of detector SNR degradation D (defined in Eq. 24) versus loop SNR. The degradation in SNR is slightly larger for the absolute-value detector than for the square-law detector when tracking a square wave, but less when tracking a sine wave, and it can be as large as 3 dB depending on the operating parameters.

The results are summarized in Figs. 7 and 8. The detector SNR as a function of E_s/N_0 is shown in Fig. 7 for both infinite and 15-dB loop SNR, and for $W = 1.0$ and 0.25. When $W = 1$, a good rule of thumb is that the detector SNR varies linearly with E_s/N_0, with slope equal to 2/3 on a decibel scale. For different values of M, the curve will be scaled vertically in a linear fashion. Figure 8 depicts the detection probability for the square-law and absolute-value detectors respectively, as a function of E_s/N_0 for both infinite and 15-dB loop SNR. The conclusion from Fig. 8 is that when operating at low loop SNR (i.e., 15 dB), an extra 1.5-dB increase in E_s/N_0 or a comparable increase in M will achieve the detection probability which was designed for assuming infinite loop SNR.

For design purposes, Fig. 9 can be useful since it depicts both the detection probability and the required threshold as a function of M for both detectors. As a design example, suppose that the absolute-value detector is required to operate at $P_f = 10^{-4}$ and $P_d = 0.99$, and that the signal is a square wave with symbol rate $\tau_s = 80$ symbols per second, $E_s/N_0 = 0.0$ dB, and loop SNR = 15 dB with a quarter window ($W = 0.25$). Figure 9 indicates that at least 90 detector samples (y_k) are needed to achieve 0.99 probability of detection.

Setting $M = 100$ (integration time = 1.25 sec), τ is obtained using Eqs. (21) and (22), with $P_f = 10^{-4}$. Figure 9 predicts that τ should be set to 46, assuming that the outputs of the integrate-and-dump devices are scaled by the factor $1/\sqrt{2\sigma_n^2 L}$. Using Fig. 7 ($M = 30$), one can check that when the detector is in-lock, $\mathrm{SNR}_z \approx 13 + 10\log_{10}(100/30) = 16.3$ dB, where scaling was performed to extend the results of Fig. 7 for $M = 100$. This is confirmed in Fig. 5, which depicts $P_d = 0.99$ for $\mathrm{SNR}_z \approx 16$ dB.

IV. Conclusion

This article presents a mathematical model of the performance of two lock detectors for Costas loops: the square-law detector and the absolute-value detector. The model concentrates on the impact of phase jitter in the tracking loop on the performance of the lock detectors. Results of the analysis were verified by computer simulation and show that low loop SNRs result in a degradation in probability of lock detection, the amount of which is dependent on the scenario of interest. That decrease can be overcome by properly readjusting the design parameters. It was further shown that the square-law detector experiences less degradation due to phase jitter than the abolute-value detector, and that the degradation in detector signal-to-noise ratio is more pronounced for square-wave than for sine-wave signals.

Acknowledgments

The authors acknowledge Dr. Marvin Simon of Section 339 and Fred Krogh and William Snyder of Section 366 for their helpful discussions during the preparation of this article.

References

[1] J. Yuen, *Deep Space Telecommunications Systems Engineering*, New York: Plenum Press, 1983.

[2] W. C. Lindsey, *Synchronization Systems in Communication and Control*, New Jersey: Prentice-Hall, 1972.

[3] G. L. Hedin, J. K. Holmes, W. C. Lindsey, and K. T. Woo, "Theory of False Lock in Costas Loops," *IEEE Trans. on Comm.*, vol. COM-26, no. 1, pp. 1-12, January 1978.

[4] S. T. Kleinberg and H. Chang, "Sideband False-Lock Performance of Squaring, Fourth-Power, and Quadriphase Costas Loops for NRZ Data Signals," *IEEE Trans. on Comm.*, vol. COM-28, no. 8, pp. 1335-1342, August 1980.

[5] M. L. Olson, "False Lock Detection in Costas Demodulators," *IEEE Trans. on AES*, vol. AES-11, pp. 180-182, March 1975.

[6] W. Hurd and S. Aguirre, "A Method to Dramatically Improve Subcarrier Tracking," *IEEE Trans. on Comm.*, vol. COM-36, no. 2, pp. 238-243, February 1988.

[7] W. C. Lindsey and M. K. Simon, *Telecommunication Systems Engineering*, New Jersey: Prentice-Hall, 1973.

[8] M. K. Simon, "On the Optimality of the MAP Estimation Loop for Carrier Phase Tracking BPSK and QPSK Signals," *IEEE Trans on Comm.*, vol. COM-27, no. 1, pp. 158-165, January 1979.

[9] J. K. Holmes, *Coherent Spread Spectrum Systems*, New York: John Wiley and Sons, 1982.

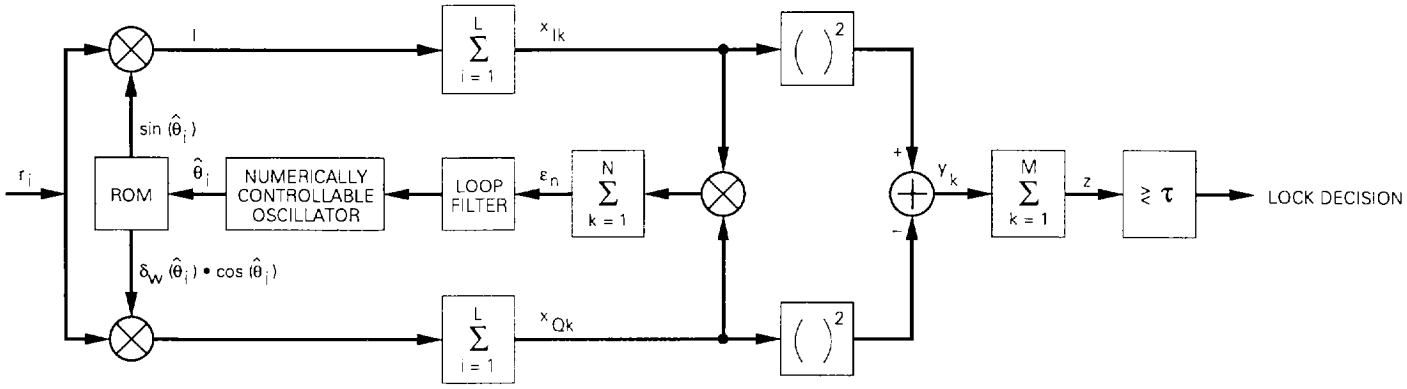

Fig. 1. Costas loop with the square-law detector.

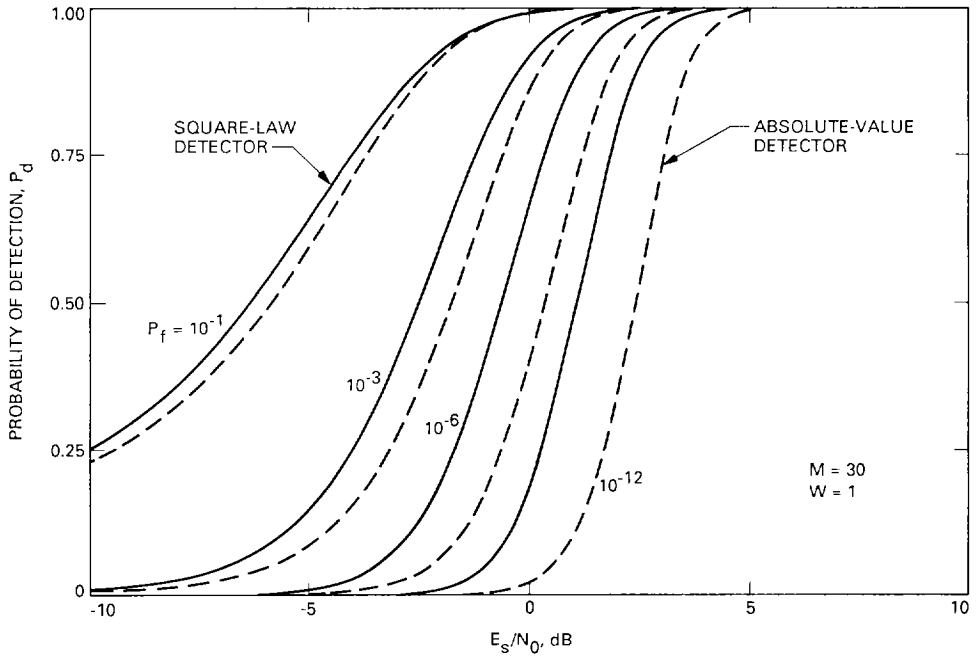

Fig. 2. Probability of detection versus E_s/N_0, infinite loop SNR, sine wave and square wave.

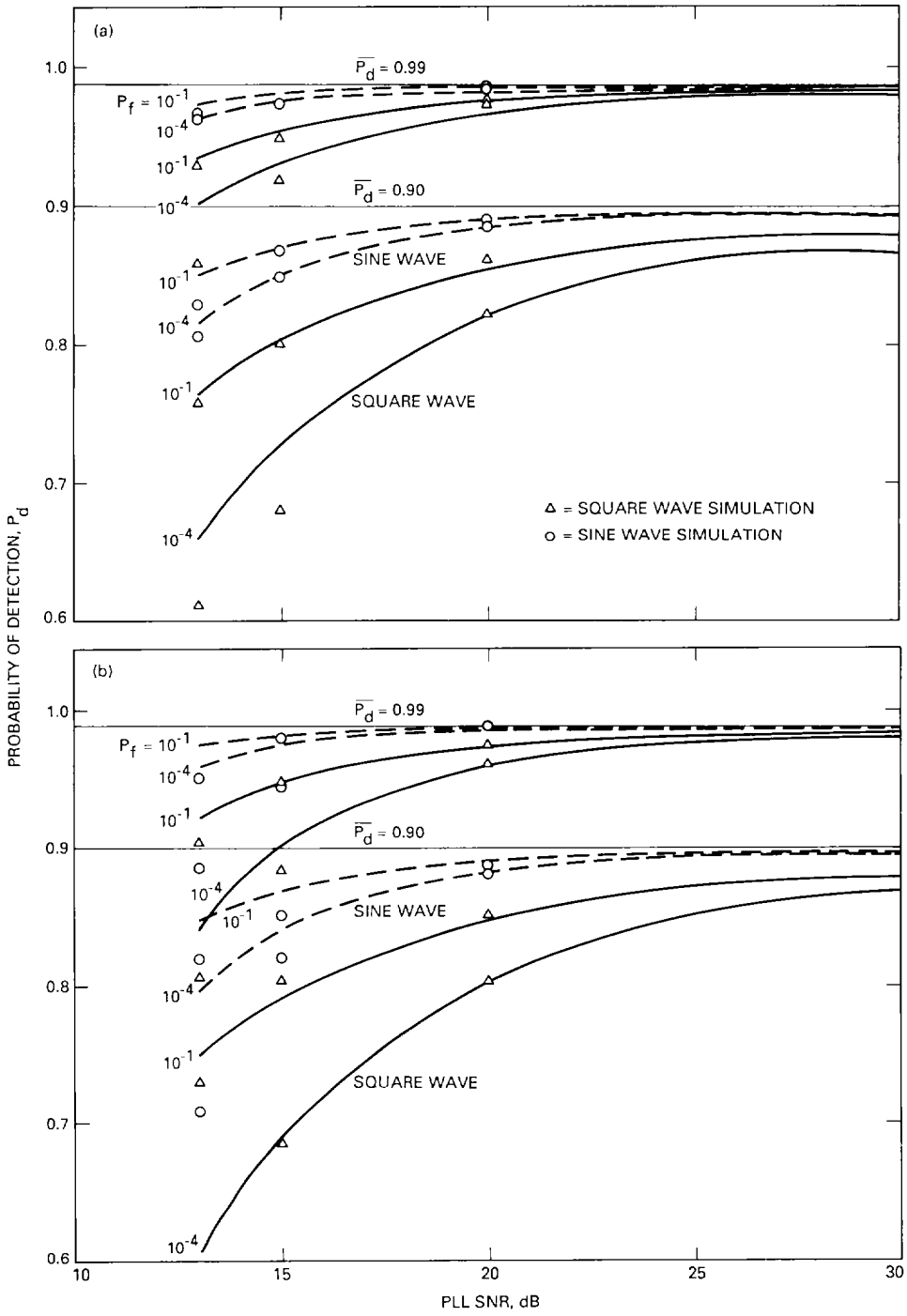

Fig. 3. Probability of detection versus loop SNR: (a) square-law detector, (b) absolute-value detector.

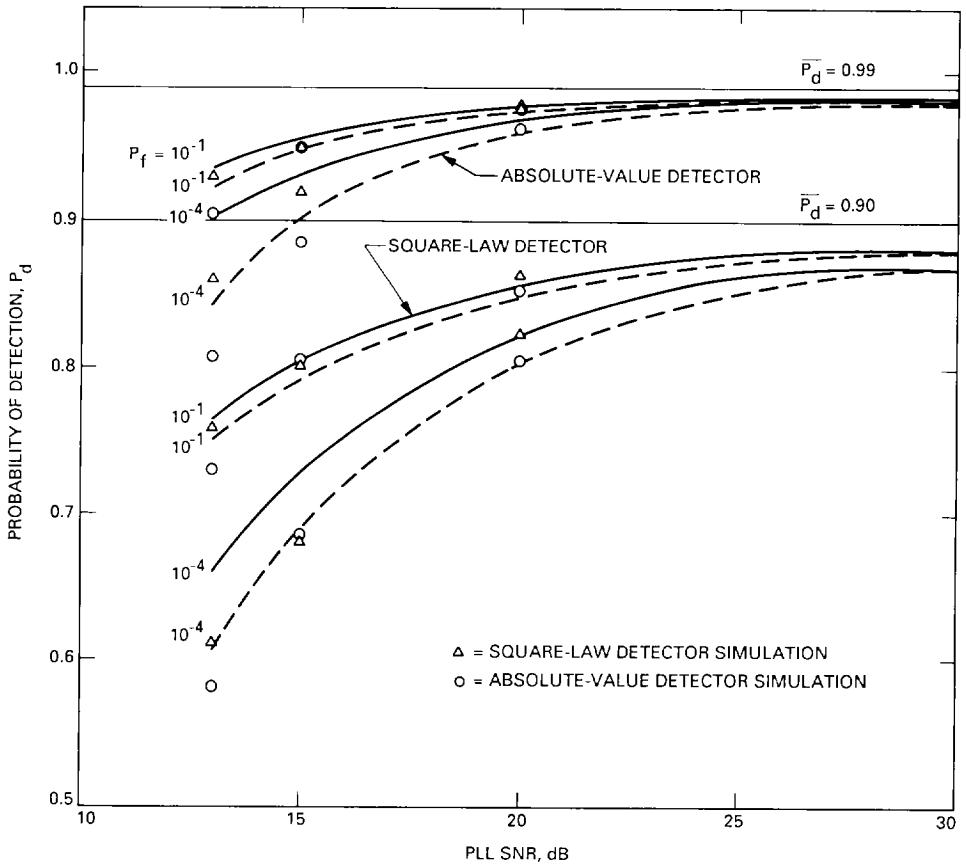

Fig. 4. Probability of detection versus loop SNR, square wave.

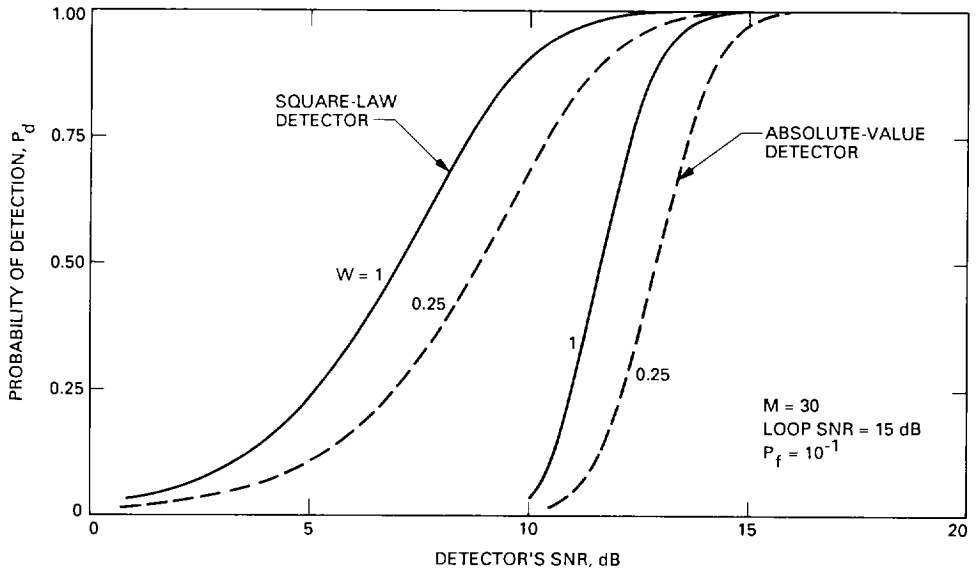

Fig. 5. Probability of detection versus detector's SNR.

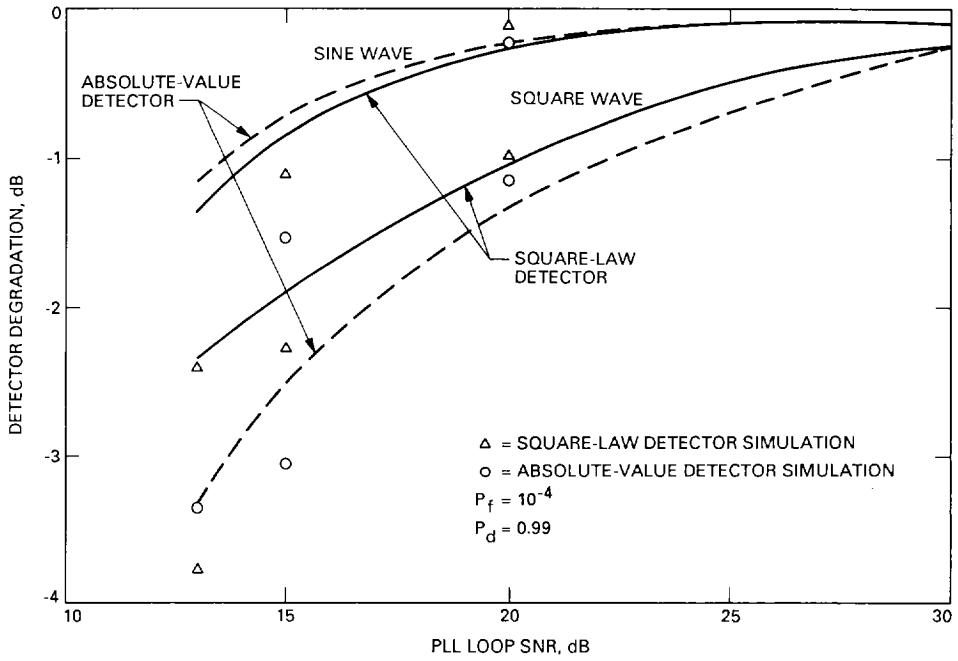

Fig. 6. Detector degradation versus phase-locked-loop SNR.

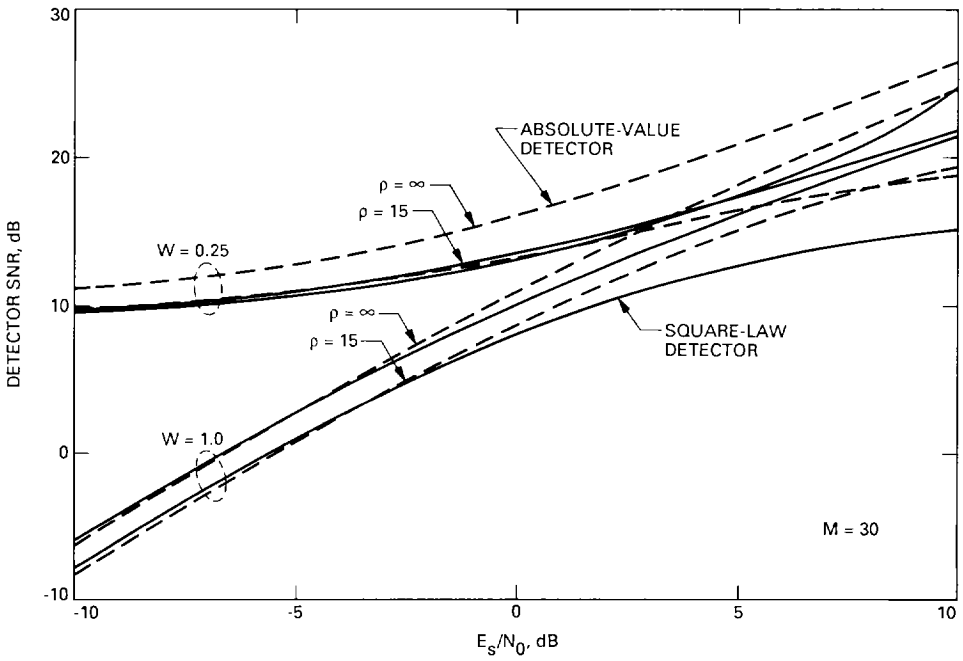

Fig. 7. Detector's SNR versus E_s/N_0.

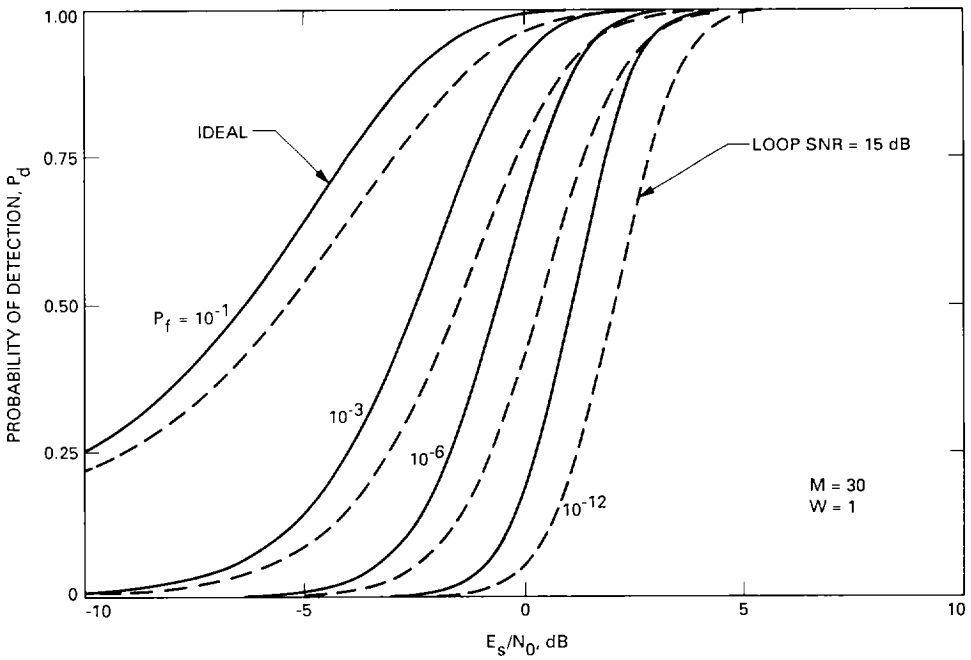

Fig. 8. Probability of detection versus E_s/N_0.

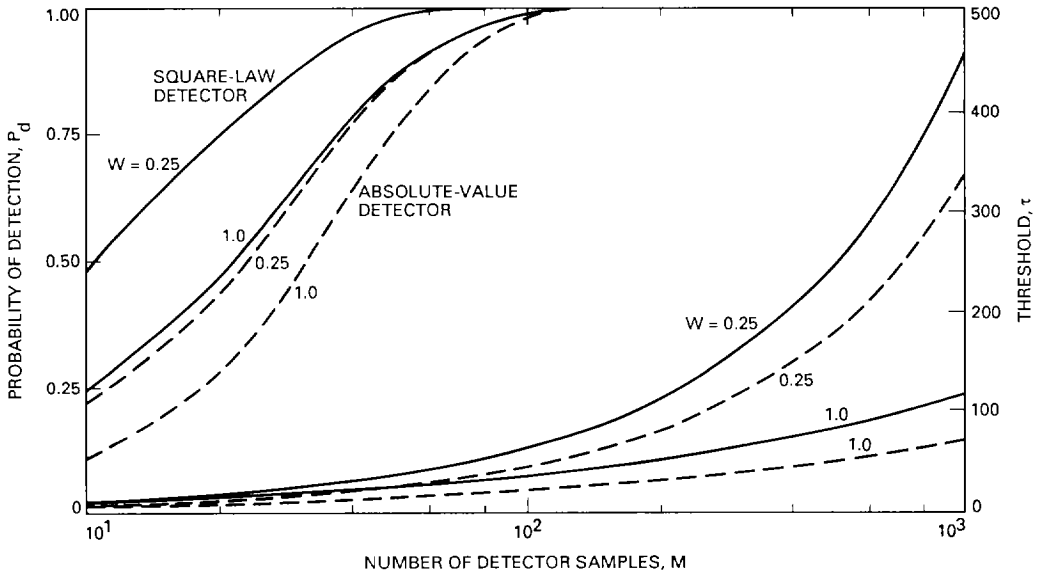

Fig. 9. Probability of detection and threshold τ versus number of detector samples M.

Appendix

Derivation of Detector's First Two Moments at Low Loop SNR

A. Square-Law Detector

Using Eq. (5) with Eq. (4), the expression for lock-detector signal is rewritten as follows

$$\begin{aligned} y_k &= L^2 P_D \left(\omega_k^2 - v_k^2\right) + \left(n_{Ik}^2 - n_{Qk}^2\right) \\ &\quad + 2 d_k L \sqrt{P_D}\ \left(\omega_k n_{Ik} - v_k n_{Qk}\right) \\ &= a_k + b_k + c_k \\ z &= \sum_{k=1}^{M} \left(a_k + b_k + c_k\right) \end{aligned} \tag{A-1}$$

To assess the performance of the lock detector, the first two moments of z are needed. For a square-wave subcarrier, $\omega_k^2 - v_k^2 = 1 - \frac{4}{\pi} \mid \phi_k \mid$, and for a sine-wave subcarrier, $\omega_k^2 - v_k^2 = \cos 2\phi_k$. Assuming that ϕ is a zero-mean (no Doppler) Gaussian phase process, it can be shown that

$$\overline{\mid \phi_k \mid} = \sqrt{\frac{2}{\pi}} \sigma_\phi \left(1 - \exp\left(-\frac{b^2}{2\sigma_\phi^2}\right)\right) \tag{A-2}$$

and

$$\overline{\phi_k^2} = \sigma_\phi^2 \operatorname{erf}\left(\frac{b}{\sqrt{2\sigma_\phi^2}}\right) - \frac{2}{\pi}\, \sigma_\phi b \exp\left(-\frac{b^2}{2\sigma_\phi^2}\right) \tag{A-3}$$

where $b \triangleq \frac{W\pi}{2}$, σ_ϕ^2 is the variance of the phase-jitter process in the subcarrier loop, and erf (x) is the error function defined as

$$\operatorname{erf}(x) \triangleq \frac{2}{\sqrt{\pi}} \int_0^x \exp\left(-t^2\right) dt$$

At first glance, Eq. (A-3) seems to express the variance of the phase-error process as a nonlinear function of itself. This is not the case since $\overline{\phi_k^2}$ is the variance in the window of the loop, and σ_ϕ^2 is the variance integrated over the complete density. This subtle effect is due to the Gaussian assumption, which approximates a density over a finite interval by the Gaussian density which is over an infinite interval. Numerically, $\overline{\phi_k^2}$ and σ_ϕ^2 are very close for all practical values of loop SNR. Note that the moments of Eqs. (A-2) and (A-3) are independent of k. The expected value of z is

$$\mu_z = M\left(L^2 P_D d + L\sigma_n^2 (1 - W)\right) \tag{A-4}$$

where d is the signal degradation factor due to phase jitter in the tracking loop, and $\overline{c_k} = 0$. Using Eq. (A-2) results in

$$d = 1 - 2\left(\frac{2}{\pi}\right)^{1.5} \sigma_\phi \left(1 - \exp\left(-\frac{b^2}{2\sigma_\phi^2}\right)\right)$$

for a square-wave subcarrier, and

$$d = \exp\left(-2\sigma_\phi^2\right)$$

for a sine-wave subcarrier. To compute the variance of z, Eq. (A-1) is used to get

$$\begin{aligned} z^2 &= A \sum_{i=1}^{M} \sum_{j=1}^{M} g_i g_j + \sum_{i=1}^{M} \sum_{j=1}^{M} \left(n_{Ii}^2 - n_{Qi}^2\right)\left(n_{Ij}^2 - n_{Qj}^2\right) \\ &\quad + B \sum_{i=1}^{M} \left(\omega_k n_{Ii} - v_k n_{Qi}\right)^2 + C \sum_{i=1}^{M} \sum_{j=1}^{M} g_i \left(n_{Ij}^2 - n_{Qj}^2\right) \end{aligned}$$

where $A = L^4 P_D^2$, $B = 4L^2 P_D$, $C = 2L^2 P_D$, and $g_i = (\omega_i^2 - v_i^2) = (1 - \frac{4}{\pi} \mid \phi_i \mid)$ for a square-wave subcarrier. In the above equation, six terms were left out because their expected value is zero. Taking the expected value of z^2, first over the thermal noise, and second over the phase process in the tracking loop, the following is obtained:

$$\begin{aligned} \overline{z^2} &= L^4 P_D^2 M^2 g + 2ML^2 \sigma_n^4 (1 + W^2) \\ &\quad + M^2 L^2 \sigma_n^4 (1 - W)^2 \\ &\quad + 4ML^3 P_D \sigma_n^2 (f + hW) \\ &\quad + 2M^2 L^3 \sigma_n^2 (1 - W) d \end{aligned} \tag{A-5}$$

where

$$g = \frac{1}{M^2} \sum_{i=1}^{M} \sum_{j=1}^{M} \overline{g_i g_j}$$

and f, h are given by

$$f = \overline{\omega_k^2} = \left(1 - \frac{4}{\pi} \overline{|\phi|} + \frac{4}{\pi^2} \overline{\phi^2}\right)$$
$$h = \overline{v_k^2} = \frac{4}{\pi^2} \overline{\phi^2} \tag{A-6}$$

for a square-wave subcarrier and

$$f = \overline{\omega_k^2} = \overline{\cos^2 \phi} = 0.5\left(1 + \exp(-2\sigma_\phi^2)\right)$$
$$h = \overline{\sin^2 \phi} = 0.5\left(1 - \exp(-2\sigma_\phi^2)\right) \tag{A-7}$$

for a sine-wave subcarrier. The variance of z can be found from the relation $\sigma_z^2 = \overline{z^2} - (\overline{z})^2$. Using Eqs. (A-4) and (A-5) results in

$$\sigma_z^2 = M^2 L^4 P_D^2 (g - d^2) + 4ML^3 P_D \sigma_n^2 (f + hW) + 2ML^2 \sigma_n^4 (1 + W^2) \tag{A-8}$$

Note that at high loop SNR, $g \to 1$, $d \to 1$, $f \to 1$, $h \to 0$, and Eqs. (A-4) and (A-8) reduce to

$$\mu_z = ML^2 P_D + ML\sigma_n^2 (1 - W)$$
$$\sigma_z^2 = 4ML^2 \sigma_n^4 \left[\frac{LP_D}{\sigma_n^2} + \frac{1 + W^2}{2}\right]$$

as they should. In order to evaluate g, one must know the correlation between samples of the phase-error process in the tracking loop. That was obtained by simulation and is shown in Fig. A-1. A good closed-form model is given by

$$R(\tau) = \sigma_\phi^2 C(\tau) \tag{A-9a}$$

where

$$C(\tau) = \left(1 - \frac{|B_L \tau|}{0.91}\right) \exp(-1.25 B_L \tau) \tag{A-9b}$$

and where σ_ϕ^2 is the closed-loop variance of the phase process and B_L is the one-sided loop bandwidth. In order to evaluate g, one needs to know the second-order joint density function of the phase-error process $p(\phi_i, \phi_j, \tau)$. As an approximation, it is assumed to be a two-dimensional Gaussian density specified by the means, variances, and correlation coefficient $R(\tau)$, which is obtained by simulation. Hence,

$$p(\phi_i, \phi_j, \tau) \approx \frac{1}{2\pi\sqrt{R^2(0) - R^2(\tau)}} \exp\left(-\frac{R(0)\phi_i^2 - 2R(\tau)\phi_i\phi_j + R(0)\phi_j^2}{2\left(R^2(0) - R^2(\tau)\right)}\right)$$
$$= \frac{1}{2\pi\sigma_\phi^2\sqrt{1 - C^2(\tau)}} \exp\left(-\frac{\phi_i^2 - 2C(\tau)\phi_i\phi_j + \phi_j^2}{2\sigma_\phi^2\left(1 - C^2(\tau)\right)}\right) \tag{A-10}$$

Here g can be evaluated from the following:

$$g = \frac{1}{M^2} \sum_{i=1}^{M} \sum_{j=1}^{M} \int_{-b}^{b} \int_{-b}^{b} g_i g_j p(\phi_i, \phi_j, \tau_{ij}) d\phi_i d\phi_j \tag{A-11}$$
$$\tau_{ij} = T_L(i - j) = t_i - t_j$$

Expanding Eq. (A-11) for the square-wave subcarrier results in

$$g = \left(1 - \frac{8}{\pi} \overline{|\phi|} + \left(\frac{4}{\pi}\right)^2 s\right)$$

where

$$s = \frac{1}{M^2} \sum_{i=1}^{M} \sum_{j=1}^{M} \int_{-b}^{b} \int_{-b}^{b} |\phi_1| |\phi_2| p(\phi_1, \phi_2, \tau_{ij}) d\phi_1 d\phi_2 \tag{A-12}$$

The correlation function in Eq. (A-10) is symmetric, i.e, $R(\tau_{ij}) = R(\tau_{ji})$, and depends only on the magnitude of the difference $k = |i - j|$. This property allows the double summation in Eq. (A-12) to be reduced to a single summation:

$$s = \frac{1}{M^2} \sum_{k=0}^{M-1} c(k) d(k)$$

where $c(0) = M$, $c(k) = 2(M-k)$ for $k = 1, 2, \ldots, M-1$, and

$$d(k) = \int_{-b}^{b} \int_{-b}^{b} \mid \phi_1 \mid\mid \phi_2 \mid p(\phi_1, \phi_2, \tau_k) d\phi_1 d\phi_2$$

Note that $\sum_{k=0}^{M-1} c(k) = M^2$ as it should. For $k = 0$, the above probability density function (pdf) reduces to a delta function times a zero-mean Gaussian pdf with variance σ_ϕ^2, so that

$$\overline{\mid \phi_1 \mid\mid \phi_2 \mid} = \sigma_\phi^2$$

Because

$$\overline{\mid \phi \mid} \approx \sqrt{\frac{2}{\pi}} \sigma_\phi$$

the first term of Eq. (A-8) can be rewritten as follows:

$$\sigma_{z1}^2 = M^2 L^4 P_D^2 \left(\frac{4}{\pi}\right)^2 \left(s - \frac{2}{\pi}\sigma_\phi^2\right)$$

It can be shown that the lower bound of the above equation equals

$$\sigma_{z1}^2 = M L^4 P_D^2 \left(\frac{4}{\pi}\right)^2 \left(1 - \frac{2}{\pi}\right) \sigma_\phi^2$$

Keeping all detector parameters constant, as the loop SNR decreases (i.e., σ_ϕ^2 increases), μ_z, σ_z^2, SNR_z, P_f, and P_d decrease.

For a sine-wave subcarrier,

$$g = \frac{1}{M^2} \sum_{k=0}^{M-1} c(k) d(k)$$

where $c(k)$ is the same as in the square-wave subcarrier case, and

$$d(k) = \begin{cases} 0.5\left(1 + \exp(-2\sigma_\phi^2)\right) & \text{for } k = 0 \\ \exp(-4\sigma_\phi^2) \cosh\left(2\sigma_\phi^2 C(\tau_k)\right) & k = 1, 2, \ldots, M-1 \end{cases}$$

B. Absolute-Value Detector

At low SNR in the tracking loop, the mean value of the detector's signal z is obtained by taking the expected value of y_k (Eq. 15) over the phase process in the tracking loop, and multiplying the result by M (the number of y_k samples):

$$\mu_z = M\left(\overline{r_{Ik}} - \overline{r_{Qk}}\right)$$

$$= M\left[L\sqrt{P_D}\left(\overline{\omega \operatorname{erf}\left(\sqrt{\frac{E_s}{N_0}\omega^2}\right)} - \overline{v \operatorname{erf}\left(\sqrt{\frac{E_s v^2}{N_0 W}}\right)}\right)\right.$$

$$\left. + \sqrt{\frac{2L}{\pi}}\sigma_n\left(\overline{\exp\left(-\frac{E_s}{N_0}\omega^2\right)} - \sqrt{W}\,\overline{\exp\left(-\frac{E_s}{N_0}\frac{v^2}{W}\right)}\right)\right]$$

where ω and v are defined by Eq. (2) or Eq. (3), and r_{Ik} and r_{Qk} are defined by Eq. (14). The variance of z is obtained from $\sigma_z^2 = \overline{z^2} - \overline{z}^2$, namely

$$\sigma_z^2 = \sum_{i=1}^{M}\sum_{j=1}^{M} \overline{\mid x_{Ij} \mid\mid x_{Ij} \mid} + \sum_{i=1}^{M}\sum_{j=1}^{M} \overline{\mid x_{Qj} \mid\mid x_{Qj} \mid}$$

$$- 2\sum_{i=1}^{M}\sum_{j=1}^{M} \overline{\mid x_{Ij} \mid\mid x_{Qj} \mid} - \left(\sum_{i=1}^{M} \overline{\mid x_{Ij} \mid} - \overline{\mid x_{Qi} \mid}\right)^2$$

The following is now obtained:

$$\sigma_z^2 = M\left(L^2 P_D\left(\overline{\omega^2} + \overline{v^2}\right) + L\sigma_n^2(1+W)\right)$$

$$+ \sum_{\substack{\text{all } i,j \\ i \neq j}}\sum \left(\overline{r_{Ii} r_{Ij}} + \overline{r_{Qi} r_{Qj}}\right) - M^2\left(\overline{r_I}^2 + \overline{r_Q}^2\right)$$

where again r_I and r_Q are defined by Eq. (14). Unfortunately, closed-form solutions for most of the above equations are not obtainable and their evaluation has to be done numerically.

The double sum in the above equation equals

$$s = \sum_{k=1}^{M-1} c(k) d(k)$$

where $c(k) = 2(M-k)$ for $k = 1, 2, \ldots, M-1$, and

$$d(k) = \int_{-b}^{b} \int_{-b}^{b} \left[r_I(\phi_1) r_I(\phi_2) + r_Q(\phi_1) r_Q(\phi_2) \right] \times p(\phi_1, \phi_2, \tau_k) d\phi_1 d\phi_2$$

where the probability density function is again approximated by Eq. (A-10). An upper bound of σ_z^2 is

$$M\left(L^2 P_D + L\sigma_n^2(1+W) - \left(\overline{r_I}^2 + \overline{r_Q}^2\right)\right)$$

and a lower bound is

$$M\left(L^2 P_D(f+h) + L\sigma_n^2(1+W) - \left(\overline{r_I}^2 + \overline{r_Q}^2\right)\right)$$

where f and h are defined in Eqs. (A-6) and (A-7).

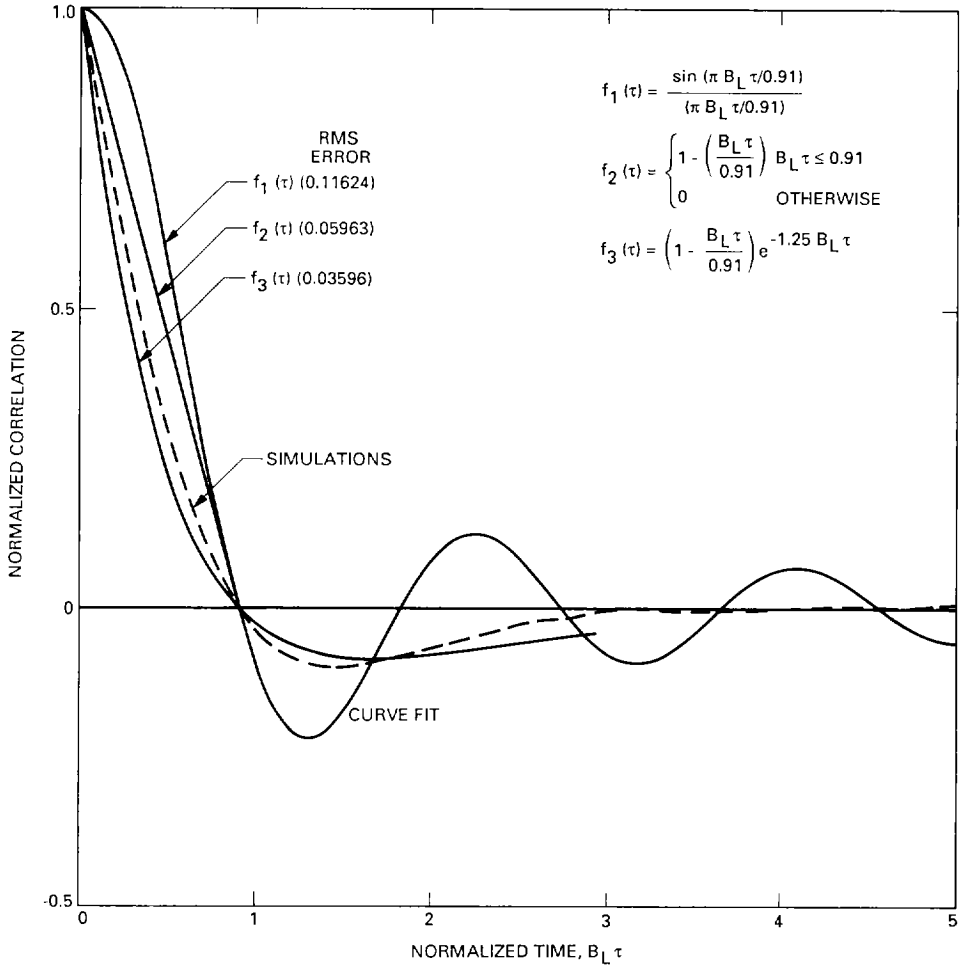

Fig. A-1. Correlation function of the phase process.